

Adsorption of Hexavalent Chromium from Aqueous Medium Using a New Schiff Base Chitosan Derivative

¹Balakrishna Prabhu K., ²M.B. Saidutta and ³M. Srinivas Kini

¹Department of Chemical Engineering, Manipal Institute of Technology, Manipal, Karnataka State, India.

*Corresponding author

²Department of Chemical Engineering, National Institute of Technology Karnataka, Mangaluru, India.

³Department of Chemical Engineering, Manipal Institute of Technology, Manipal, Karnataka, India.

^{1,2,3}ORCID: 0000-0002-7920-8968; 0000-0003-0683-6370; 0000-0001-6408-0538

Abstract

Modification of chitosan biopolymer was achieved by grafting (3-phenyl-1H-pyrazole-4-carbaldehyde) by the Schiff base reaction to synthesize a new chitosan derivative (ChD). The formation of the product was confirmed by FTIR, XRD and ¹³CNMR analysis. The grafted molecule provided additional nitrogen bearing groups as binding sites. The new derivative was used to investigate the removal of Cr (VI) ions in water. The sorption was best favoured at a pH of 3.0. From the Langmuir isotherm, the maximum monolayer adsorption capacity for the adsorbent was determined ($Q_0=63.5$ mg/g). The sorption data fitted satisfactorily to the Redlich-Peterson isotherm. The kinetics of adsorption was best described by pseudo-second order rate equation. The thermodynamic study revealed that the adsorption of Cr (VI) on to ChD was spontaneous and accompanied by increase in entropy. The metal removal was favoured at lower temperatures indicating that the adsorption was exothermic in nature.

Keywords : Chitosan, adsorption, chitosan-derivative, chromium removal

Chromium is a toxic metal pollutant which is often a part of the waste discharged from diverse industries such as petroleum refining, mining, leather, textiles, electroplating, aluminium processing, inorganic chemicals, dyes and pigment [1][2]. Like most transition metals, chromium can exist in six oxidation states. In aerated aqueous media only the Cr (III) and Cr (VI) are stable [3]. Cr (III) is the most common form encountered in natural aquatic media; it is a micronutrient which is essential for sugar and fat metabolism in organisms [4]. Virtually all Cr (VI) present in aquatic bodies owe their presence to anthropogenic activities. Cr (VI) travels quickly through food chain and is more harmful than Cr (III); it can cause skin irritation, liver damage, pulmonary congestion and ulcer

formation; its cancer causing nature, reproductive and developmental toxicity and neurotoxicity are well documented [5] [6] [7] [8]. Therefore, attention to hexavalent than trivalent chromium is of prime importance in water pollution abatement [9]. The World Health Organization (WHO), as per its drinking water guidelines, has set the highest permissible amount of total chromium as 50µg/L [10]. Chromium is removed from polluted water by several processes such as electrochemical precipitation, ion exchange, membrane separation, solvent extraction, evaporation and adsorption [11]. Adsorption techniques have been very effectively used for recovering and eliminating heavy metals from dilute solutions [12].

Recently chitosan (CS) has been keenly studied for removal of heavy metals due to its excellent ability for complexing metal ions. Chitosan exhibits many advantageous features such as biocompatibility, biodegradability, renewability, bioactivity, and non-toxicity [13] [14] [15] [16]. The adsorption behaviour of chitosan can be augmented by simple chemical modifications [17]. To improve adsorption capacity, in addition to cross-linking, researchers have employed diverse chemical modifications that include addition of new functional groups and conditioning of chitosan beads [18] [19].

Inserting groups containing nitrogen atoms into the chitosan polymer chain provides additional binding sites for protonation under acidic conditions whereby enhanced removal of Cr (VI) can occur primarily by the mechanism of electrostatic attraction. The synthesized chitosan derivative (ChD) has a pyrazole ring with additional nitrogen atoms. In this study, chitosan derivative [3-phenyl-1H-pyrazole-4-carbaldehyde-chitosan] (ChD) was synthesized, characterised and its effectiveness in sorptive elimination of Cr (VI) has been investigated.

MATERIALS AND METHODS

Materials

Chitosan powder (30 mesh) having 90 % deacetylation was procured from Seafresh Industry Public Co., Ltd. Thailand. All chemicals used were of analytical reagent grade.

Stock solution of 1000 mg/L of Cr (VI) was prepared by dissolving $K_2Cr_2O_7$ (Thomas Baker) in double distilled water. Solutions of lower concentrations required were prepared by diluting this solution with double distilled water. The concentrations were validated by AAS.

Synthesis of ligand [3-phenyl-1H-pyrazole-4-carbaldehyde]

The pyrazole based ligand [3-phenyl-1H-pyrazole-4-carbaldehyde] was synthesized in two stages as described in literature [20][21].

In the first step semicarbazone was synthesized by refluxing a mixture of acetophenone (15.6 mL, 0.13 mol), semicarbazide hydrochloride (13.38g, 0.12 mol) and sodium acetate (16.32g, 0.20 mol) in 125 mL ethanol taken in a 1L round-bottom flask for 4h. The reaction mixture was cooled to room temperature and filtered. The off white precipitate was washed in ethanol to remove organic impurities, filtered and then washed with distilled water. After filtration, the precipitate semicarbazone was dried overnight at 50°C. Phosphorous oxychloride (19.8 mL, 0.21mol) was taken with dimethyl formamide (40 mL, 0.53mol) and semicarbazone (17g, 0.097mol) was added into the flask over thirty minutes and the contents of the flask were brought to room temperature and then maintained at 80°C for 4h. The red viscous liquid was poured into a beaker having ice cold water with brisk stirring. The pH was then increased to 7.0 by adding sodium carbonate. It was then extracted with ethyl acetate in three stages using 75 mL in each stage to recover the ligand (3-phenyl-1H-pyrazole-4-carbaldehyde). The brownish yellow precipitate obtained was washed and dried at 50°C.

Synthesis of the chitosan derivative (ChD)

Chitosan powder (6g) was dissolved in 1% acetic acid (150 mL) and stirred at room temperature for one hour. Further, the thick solution was diluted by adding methanol (600 mL) and stirring was continued for an additional 16 h. Ligand (10.25g) was dissolved in chloroform (60 mL) and added to the previous mixture over a period of 10 min at room temperature following which stirring was continued for a further period of 16h at the same temperature. The reaction mixture was then heated to 60°C and maintained there with vigorous stirring for 18h. It was then brought to room temperature, thoroughly washed with 75 mL of chloroform, filtered and dried at 50°C to get the chitosan derivative ChD.

Instruments

FTIR RX-1 model by SHIMADZU was used to measure the fourier transformed infrared spectra on KBr pellets. 400MHz Solid state NMR spectrometer was used to record the ^{13}C NMR spectra. Thermo-Scientific iCE 3000 series atomic absorption spectrometer was employed to determine the Cr (VI) concentrations. Rigaku Miniflux-600 X-ray powder diffractometer was used for X-ray diffraction studies. NETZSCH DSC 404F1 differential scanning calorimeter was used to determine thermal properties. Systronics digital pH meter-335 was used to measure the pH.

Effect of pH

The effect of initial pH on adsorption was investigated by taking 25 mL of the aqueous solution of 100 mg/L conc. of Cr (VI) at different pH values (2-8) with 200 mg of sorbent. The flasks were kept in incubator shaker under agitation for 24h at 30°C at a speed of 150 rpm.

Batch studies

Aliquots of 25 mL of aqueous solutions of Cr (VI) in the conc. range of 25-1000 ppm were taken with an adsorbent dose of 100 mg. A stirring speed of 150 rpm and a temperature of 30°C were maintained during the adsorption for duration of 24 h.

Kinetic study

The kinetics of adsorption was analysed in a 250 mL Erlenmeyer flask having 125 mL of Cr (VI) solution of 100 mg/L concentration using 250 mg of ChD adsorbent. The flask was kept at 30°C and agitated at a speed of 150 rpm. Aliquots were drawn periodically, filtered and analysed by AAS.

Effect of temperature

Batch experiments were conducted at different temperatures (10-50°C) for initial concentrations of Cr (VI) ions in the 25-100 ppm range. The adsorbent dose and speed of agitation were kept constant at 2g/L and 150 rpm respectively. The data obtained was used to determine the thermodynamic parameters of adsorption.

RESULTS AND DISCUSSION

Characterization of ChD

^{13}C NMR analysis

The solid state ^{13}C NMR of chitosan showed signals at (ppm) 24.885, 58.127, 62.058, 76.158, 83.507, and 106.153. The solid state ^{13}C NMR of ChD in comparison showed additional signals

at (δ ppm)), 118.9, 132.0, 144.1, 150.3 (ArC), and 163.1 (C=N). The additional peaks confirmed the successful grafting of the ligand onto the chitosan backbone.

Fourier transform infra-red (FTIR) studies

FTIR spectra (Fig.1) uncovered the changes in the chemical structure of the neat chitosan, the modified material (ChD), and the post- adsorption ChD-Cr complex.. In the pattern of CS a broad peak around $3,600\text{ cm}^{-1}$ is assigned to the stretching vibration of O–H, the stretching vibration of N–H and the hydrogen bonding in the polymer matrix. The peak positioned around 1654 cm^{-1} is ascribed to the combined bending vibrations of C=O of the acetamide (NHCO) group, and the NH deformation of the NH_2 group. The peak at 1153 cm^{-1} is

assigned to stretching vibration in (C-O-C bridge) and the peak at 1080 cm^{-1} to (-C-O) stretching vibration in secondary alcohol (-COH) [22].

The FT-IR pattern for ChD shows a signal around 3618 cm^{-1} which is assigned to the (-OH) stretching vibrations. The band at about 1639 cm^{-1} is due to the presence of ($>\text{C}=\text{O}$) bend of acetyl units of CS-NHAc. The presence of a new peak at 1633 cm^{-1} is attributed to stretching vibrations of the imine ($>\text{C}=\text{N}-$) group [23]. The peak at 1525 cm^{-1} is assigned to bending vibration of NH of pyrazole group. The bands at 1062 cm^{-1} and 1002 cm^{-1} are assigned to the C-O stretching vibrations of the secondary and primary alcohols (C-O-H) respectively. The peak at 648 cm^{-1} is assigned to secondary wagging vibrations of NH group.

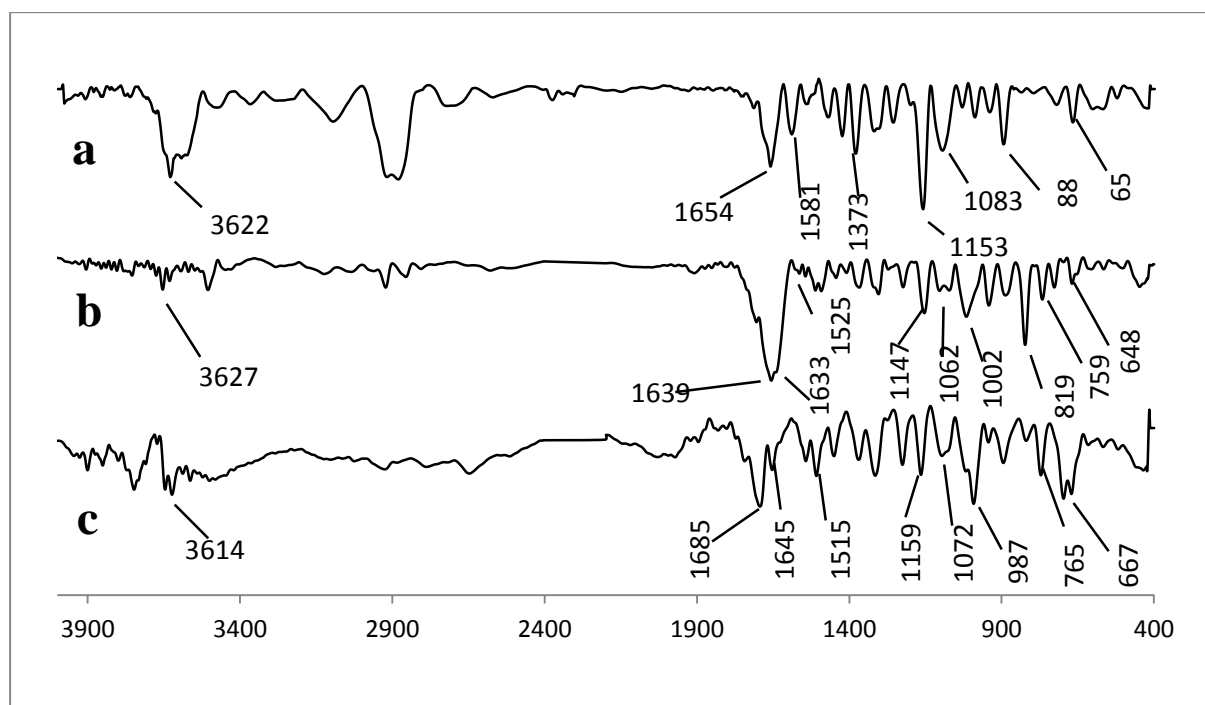


Figure 1. FTIR spectrum of (a) chitosan, (b) chitosan derivative ChD, (c) ChD-Cr(VI) complex after adsorption.

X-ray diffraction studies

The structure of ChD was investigated by X-ray diffraction at 2θ , $5-80^\circ$ with a step size of 0.02° . Fig. 2 shows the XRD pattern of CS and ChD. The diffraction pattern shows the characteristic peak at $2\theta = 10^\circ$ and $2\theta = 19^\circ, 21^\circ$. For the Schiff base, the peak at $2\theta = 10^\circ$ disappears and the distinguishing peak at around $2\theta = 20^\circ$ is of lowered intensity than that of

chitosan, based on which it is inferred that there is a decrease in the crystallinity of ChD as compared to CS. This may be owing to disruption of the strong hydrogen bond of the chitosan molecule after grafting of the ligand. The disappearance of the peak at $2\theta = 10^\circ$ is also proof of the Schiff base reaction at the NH_2 position. Similar results have been reported by other researchers [24][25][26].

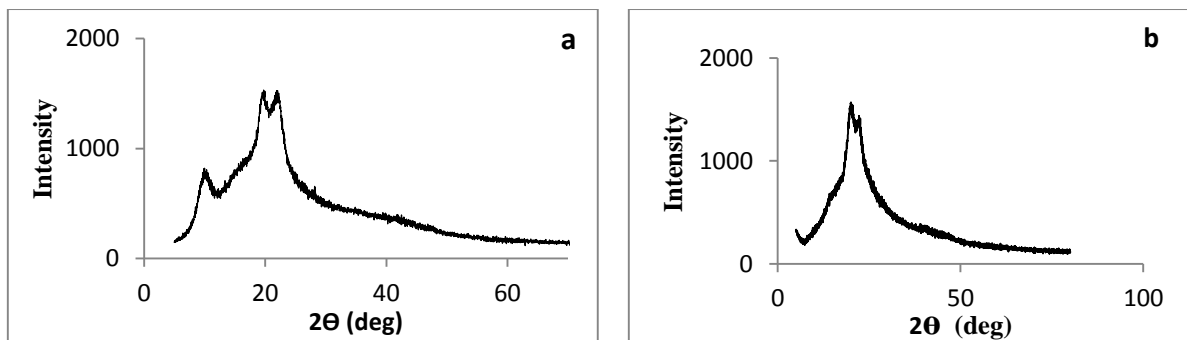
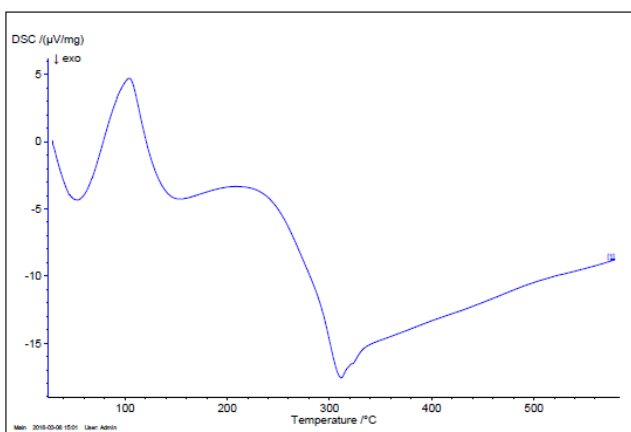


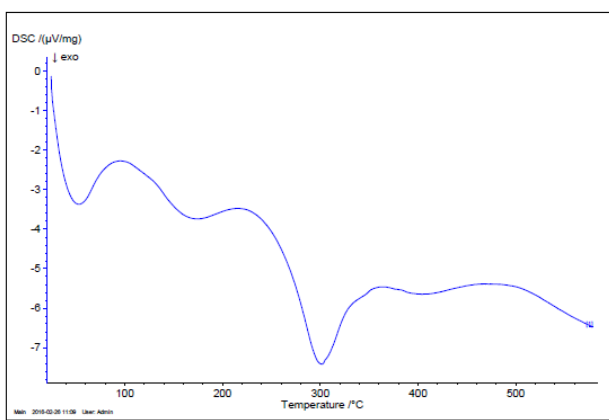
Figure 2. XRD pattern of a) chitosan b) chitosan derivative ChD

DSC thermogram studies of ChD

The DSC thermograms of CS and ChD are presented in Fig 3 a and b respectively. The thermogram for ChD shows two major exothermic peaks; a peak around 70°C is attributed to vaporisation of water present; a peak around 300°C is due to the degradation of the biopolymer derivative ChD. When the thermograms of CS and ChD are compared it is evident that the derivative ChD retains the thermal stability even after grafting of the ligand on the chitosan.



(a)



(b)

Figure 3. DSC thermogram of a) CS and b) ChD

Effect of initial pH

The removal of chromium was maximum at pH values at a pH of 3 with a removal of 73% (Fig. 4). This is consistent with reports by many other researchers employing chitosan or its derivatives where the maximum Cr (VI) removal occurred in the pH range of 2-4 [27][28][29][30]. In aqueous phase, the various anionic forms of Cr (VI) present themselves as $\text{Cr}_2\text{O}_7^{2-}$, HCrO_4^- , CrO_4^{2-} and HCr_2O_7^- depending upon the ionic concentration and pH in the solution. At low concentrations within the pH range of 2-4, the main fraction is HCrO_4^- , while the concentration of CrO_4^{2-} moiety rises with increase in pH value, turning out to be the predominant form at $\text{pH} > 7.0$ [31]. However, anions of $\text{Cr}_2\text{O}_7^{2-}$ and HCr_2O_7^- are present only at higher concentration (>1000 ppm) of Cr (VI). In the present study, at $\text{pH}=3$ and $\text{Cr (VI)} < 1000$ ppm, the predominant form is HCrO_4^- . The anions present in solution can interact with protonated amine functional groups. At low pH, electrostatic interactions between the protonated sites of the sorbent and HCrO_4^- ions support superior chromium removals. At higher pH values however, the OH^- ion competes with the oxyanions of Cr (VI) (HCrO_4^- and CrO_4^{2-}) for the protonated sites and hence the adsorption capacity decreases[32].

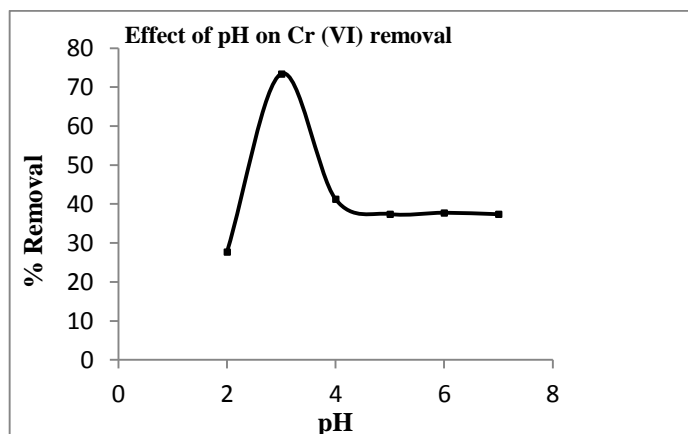


Figure 4. Effect of pH variation on % removal (Initial concentration=100 mg/L; Temperature=303 K; Ads. Dose=4g/L; Stirring speed=150 rpm; t=24h)

Adsorption isotherms

An adsorption isotherm is a mathematical correlation that explains the phenomenon of accumulation or mass transfer of a solute from the aqueous phase to a solid phase under constant temperature and pH [33]. Empirical equations play a major role in data interpretation and predictions. In this work, batch studies were carried out to validate Langmuir, Freundlich and Redlich-Peterson isotherms. The adsorption capacities under equilibrated conditions were computed from Equation 1 [34].

$$Q_e = \frac{(C_o - C_e)V}{W} \quad (1)$$

Where ' Q_e ' is the adsorption capacity of ChD (mg/g), ' V ' is the volume of the sample (L), ' C_o ' is the Cr (VI) concentration in solution (mg/L), ' C_e ' is the equilibrium Cr (VI) concentration in solution (mg/L) and ' W ' is the mass of ChD used (g).

Langmuir adsorption isotherm [35] describes adsorption occurring in a single layer, at a limited number of active sites having equal energy. The equation for the Langmuir isotherm is as shown in Equation 2.

$$Q_e = \frac{Q_o b C_e}{b C_e + 1} \quad (2)$$

Where, ' Q_o ' is the maximum monolayer adsorption capacity (mg/g) and ' b ', the Langmuir constant (L/g) linked to the adsorption energy.

The 'favourability' of adsorption is expressed by ' R_L ' a dimensionless separation parameter, which is defined as:

$$R_L = \frac{1}{1 + b C_o} \quad (3)$$

Adsorption is favourable when the value of ' R_L ' is between 0 and 1.

Freundlich isotherm [35] is an empirical model that can be applied to multilayer adsorption with varying distribution of adsorption heat and reactivity over the adsorbent surface and is given by Equation 4.

$$Q_e = K_f C_e^{1/n} \quad (4)$$

where ' K_f ' is the Freundlich adsorbent constant (mg/g)(mg/L)ⁿ and ' n ' is the dimensionless Freundlich exponent related to the ease of adsorption.

Redlich-Peterson isotherm represents adsorption equilibria over a wide concentration range, that can be applied either in homogeneous or heterogeneous systems due to its versatility [32]. The mathematical form of this isotherm is given by Equation 5.

$$Q_e = \frac{K_R C_e}{1 + a_R C_e^{b_R}} \quad (5)$$

Where, ' K_R ' (L g⁻¹), ' a_R ' (L mg⁻¹) and ' b_R ' are constants.

Table 1. Equilibrium model parameters for the adsorption of Cr (VI) on ChD

Langmuir Isotherm			Freundlich isotherm			Redlich-Peterson isotherm			
Q_o (mg g ⁻¹)	b (L mg ⁻¹)	r^2	K_f (mg g ⁻¹)	n	r^2	K_R (L g ⁻¹)	a_R (L mg ⁻¹)	b_R	r^2
63.5	0.0968	0.9390	16.445	4.440	0.9569	14.789	0.540	0.858	0.9849

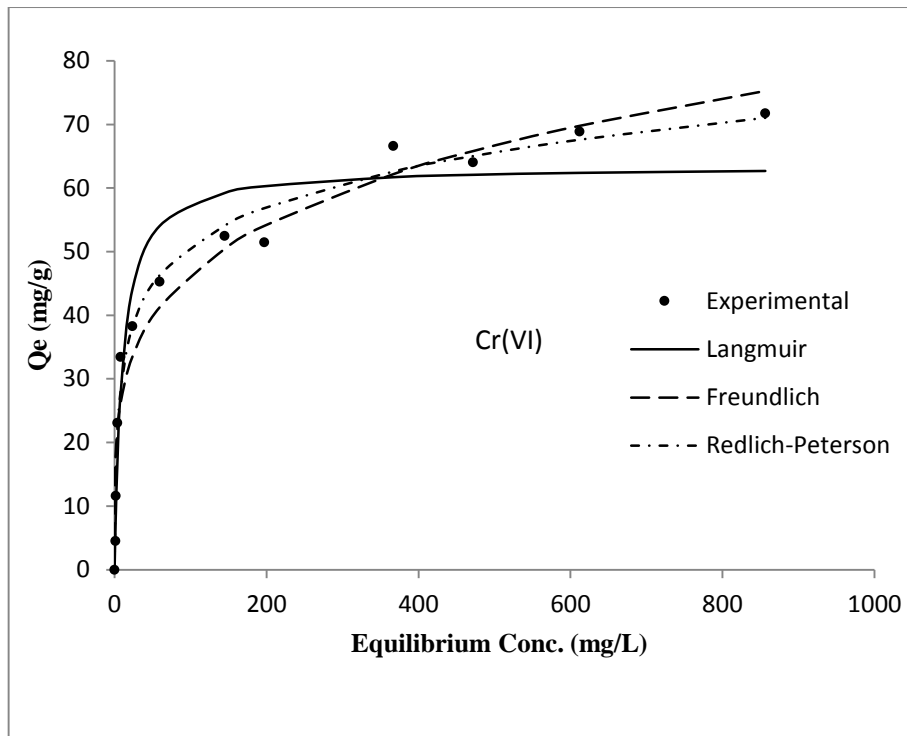


Figure 5. Plot of various adsorption isotherms to ChD-Cr (VI) adsorption data (Initial concentration=100 mg/L; Temperature=303K; pH=3; Ads. Dose=2g/L; Agitation speed=150 rpm; Contact time=24h)

The Redlich-Peterson isotherms ($r^2=0.98$) provided a better fit to the data than the Langmuir ($r^2=0.94$) and Freundlich ($r^2=0.96$) isotherms. The maximum monolayer adsorption capacity obtained was 63.46 mg/g. A comparison of adsorption capacities reported by few other researchers for Cr (VI) removal is presented in Table 2.

Table 2 Adsorption capacity of various adsorbents for Cr (VI) removal

Adsorbent	Adsorption capacity (mg/g)	Reference
Bael fruit shell	17.27	[36]
Neem leaf powder	19.49	[37]
Almond shell	10.616	[11]
Cactus	7.082	_do_
Coal	6.78	_do_
Wool	41.15	_do_
Olive cake	33.44	_do_
Pine needles	21.50	_do_
Saw dust	15.823	_do_

Jathropa oil cake	0.82	[38]
Maize corn cob	0.28	_do_
Sugarcane bagasse	0.63	_do_
Sulfonated lignite	27.12	[39]
Zr (IV)-impregnated collagen fiber	27.56	[40]
Chitosan beads	76.92	[28]
Schiff base-chitosan grafted multiwalled carbon nanotubes	95.0	[41]
Protonated cross linked chitosan beads	8.064	[42]
Carboxylated cross linked chitosan beads	9.174	(do)
Grafted cross-linked chitosan beads	13.69	(do)
Chitosan flakes	34.40	[43]
Ethylenediamine-modified cross-linked magnetic chitosan resin	51.813	[44]

Ethylenediamine modified chitosan microspheres	28.81	[27]
Chitosan modified with cellulose	13.05	[45]
Chitosan coated cotton gauze	12.4	[46]
ChD	63.456	Present work

rate constant (min^{-1}).

The pseudo-second order rate expression is expressed as follows in Equation 7 [32].

$$\frac{t}{Q_t} = \frac{t}{Q_e} + \frac{1}{k_2 Q_e^2} \quad (7)$$

In the intraparticle diffusion model the kinetic model constants are obtained by plotting quantity adsorbed against $t^{1/2}$. The model is given by Equation 8 [32].

$$Q_t = K_{id} t^{1/2} + C \quad (8)$$

Adsorption kinetics

Adsorption kinetics determines the efficiency of an adsorbent and is instrumental in determining the potential applications of an adsorbent. The pseudo-first order rate expression is expressed as given in Equation 6 [32].

$$\ln(Q_e - Q_t) = \ln(Q_e) - k_1 t \quad (6)$$

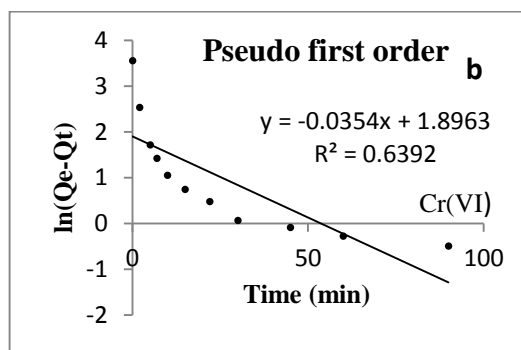
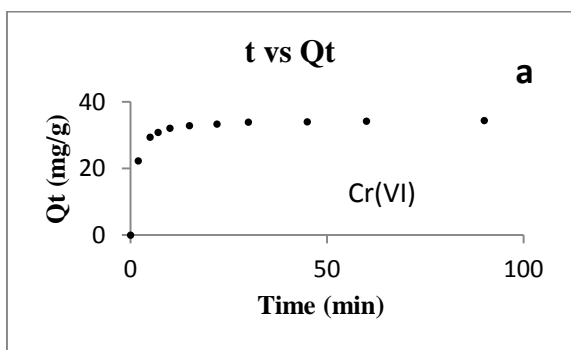
Where ' Q_e ' and ' Q_t ' are the amount adsorbed (mg/g) at equilibrium and time t (min) respectively. ' k_1 ' is the adsorption

Where, ' K_{id} ' is the intra-particle diffusion rate constant ($\text{mg/g} \cdot \text{min}^{0.5}$). If the intra-particle diffusion is the only rate-controlling step, then the plot should pass through the origin; otherwise, it signifies that the boundary layer diffusion is also important in the adsorptive interaction.

Among the three models, the pseudo second order model best represented the adsorption kinetics for ChD-Cr (VI) ($r^2=0.99$). This is presented in Table 3 and Fig. 6.

Table 3. Kinetic model fitting for adsorption of Cr (VI) to ChD

Pseudo first order				Pseudo second order				Intraparticle diffusion	
$Q_e \text{ exp}$ (mg g^{-1})	$Q_e \text{ calc}$ (mg g^{-1})	k_1 (min^{-1})	r^2	$Q_e \text{ exp}$ (mg g^{-1})	$Q_e \text{ calc}$ (mg g^{-1})	k_2 ($\text{g mg}^{-1} \text{min}^{-1}$)	r^2	K_{id} ($\text{mg g}^{-1} \text{min}^{-1/2}$)	C (mg g^{-1})
6.674	35.014	0.0354	0.6392	34.722	35.014	0.0322	0.9999	1.0426	26.832



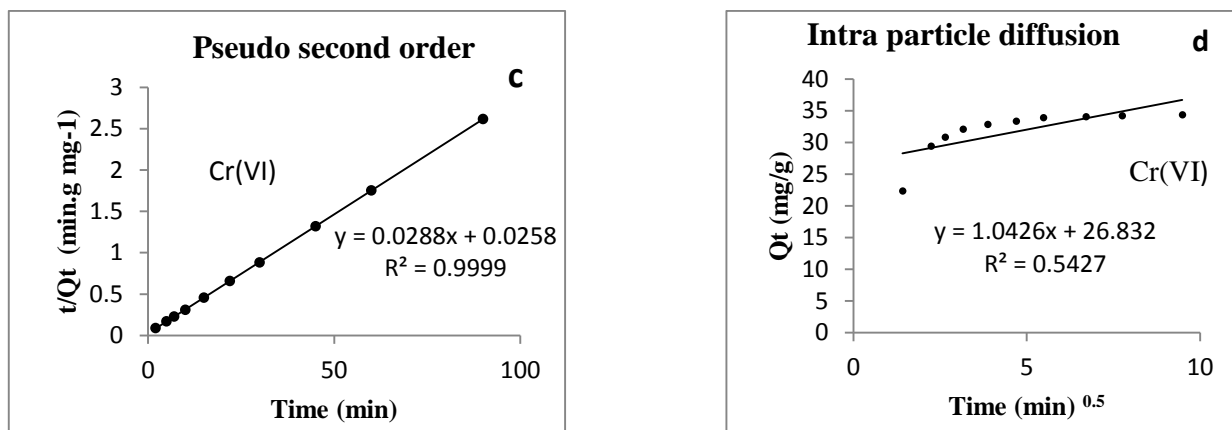


Figure 6. Plot of ChD-Cr(VI) kinetic study data [a) Quantity adsorbed v/s time b) Pseudo-first order c) Pseudo-second order d) Intra particle diffusion] (Initial concentration=100mg/L; Temperature=303K; pH=3; Ads. Dose=2g/L; Agitation speed=150rpm)

Thermodynamics

The thermodynamics of the adsorption was studied in the temperature in the range between 10°C and 50°C in intervals of 10°C.

The change in standard Gibb's free energy for adsorption is obtained by applying the well-known Van't Hoff equation given below.

$$\Delta G^{\circ} = -RT \ln K_o \quad (9)$$

where ΔG° (J/mol) is the Gibb's free energy change, R is the gas constant (J / mol K), 'T' is the temperature (K) and 'K_o' is the equilibrium constant. 'K_o' is obtained by plotting Q_e/C_e v/s

'C_e' and finding the limiting value of (Q_e/C_e) as 'C_e' tends to zero, where 'Q_e' (mg/g) is the adsorption capacity at equilibrium (mg/g) and 'C_e' (mg/mL), the metal concentration in aqueous phase at equilibrium [34].

A plot of 1/T vs ln(K_o) is then drawn and using the Equation 10, ΔS° and ΔH° can be determined [34].

$$\ln(K_o) = \frac{\Delta S^{\circ}}{R} - \frac{\Delta H^{\circ}}{RT} \quad (10)$$

The changes in standard free energy, standard enthalpy and standard entropy are presented in Table 4.

Table 4. Results of thermodynamic study for the adsorption Cr (VI) ions on ChD

Temperature (K)	K _o	ΔG° (kJ.mol ⁻¹)	ΔH° (kJ.mol ⁻¹)	ΔS° (J.mol ⁻¹ .K ⁻¹)
283.15	10499.679	-21.797	-11.606	35.514
293.15	7878.557	-21.867		
303.15	7091.839	-22.348		
313.15	6007.716	-22.653		
323.15	5639.214	-23.206		

The negative value of the change in standard Gibb's free energy indicates that adsorption is feasible and spontaneous. The negative value of the change in standard enthalpy change indicates the exothermic nature of adsorption which is favoured at lower temperatures. Positive value of change in standard entropy indicates increasing randomness and thus an affinity for the adsorbent.

Possible adsorption mechanism

At low pH values the adsorption (pH <3), the different N-atom and hydroxyl bearing groups get protonated as given in Equations 11, 12, 13 and 14 [48][49][24].





The positive electrical charges are formed on the adsorbent surface due to protonation of the various groups. The sorbate Cr (VI) which mostly exists in the form of HCrO_4^- under the experimental conditions gets attracted to these sites and the binding takes place by electrostatic interaction.

When the FTIR pattern of ChD is compared with ChD-Cr (Fig. 1), the wide band around 3618 cm^{-1} corresponding to the stretching vibrations of the hydroxyl group is shifted to 3614 cm^{-1} ; the peak at 1639 cm^{-1} ascribed to the bending vibrations of the carbonyl group ($\text{C}=\text{O}$) of

acetamide units shifts to 1685 cm^{-1} ; the absorption peak at 1633 cm^{-1} ascribed to the stretching vibrations of the imine group ($\text{C}=\text{N}$) is shifted to 1645 cm^{-1} ; the band at 1062 cm^{-1} assigned to the C-O stretching vibrations of the secondary alcohol C-O-H is shifted to 1072 cm^{-1} . Similarly, the absorption peak at 1002 cm^{-1} assigned to the C-O stretching vibrations of the primary alcohol C-O-H is shifted to 987 cm^{-1} . The band at 648 cm^{-1} assigned to the secondary wagging vibrations of the NH group is shifted to 667 cm^{-1} . From the preceding considerations, it is inferred that imine, NH and hydroxyl groups took part in the binding of Cr (VI). A schematic representation of the possible mechanism of Cr(VI) interaction with ChD is presented in Fig. 7.

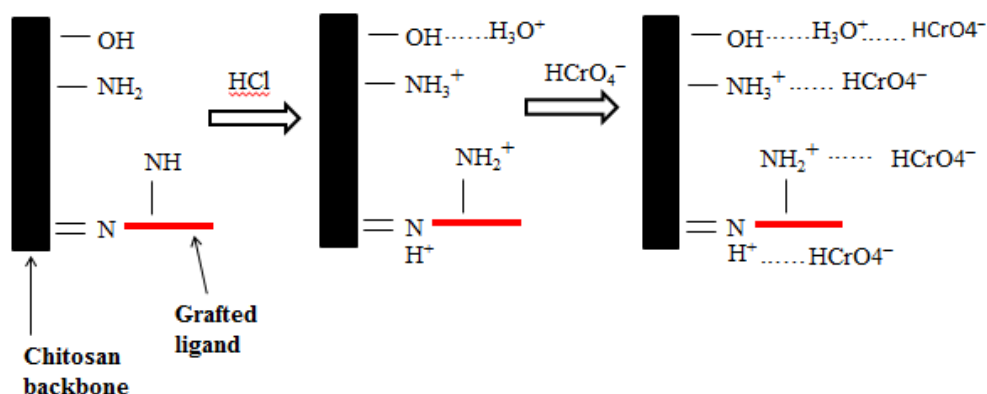


Fig.7. Possible mechanism of adsorption for the removal of Cr (VI) by ChD

CONCLUSIONS

In this work, a novel adsorbent, [3-phenyl-1H-pyrazole-4-carbaldehyde-chitosan], was successfully prepared and its effectiveness for the sorption of Cr (VI) was studied. It was observed that the removal of metal was the maximum at a pH of 3. The Redlich-Peterson model best explained the adsorption results ($r^2=0.9849$). The kinetic studies showed that the pseudo-second order model fitted the adsorption data excellently ($r^2=0.9999$). The values of ΔG° and ΔH° revealed that the adsorption process was spontaneous and exothermic. Based on FTIR analysis, the metal binding process was explained as potentially due to the mechanism of electrostatic interactions on the hydroxyl, imine and the amine groups. The findings indicate that the synthesized derivative is an effective sorbent for Cr (VI) removal.

ACKNOWLEDGEMENTS

Authors gratefully acknowledge assistance received in the form of experimental facilities for conducting this research work from Manipal University, Manipal, India. Authors are also thankful to the Director, National Institute of Technology Karnataka, India for providing the research facilities to carry

out a part of the research work reported in this article. The authors are grateful for technical help received from Dr. Arun M. Isloor, Department of Chemistry, NITK, Surathkal.

BIBLIOGRAPHY

- [1] Udy M. J. , and Lewin S.Z. Chromium, Vol. I. *Chemistry of Chromium and its Compounds*, Reinhold Publishing Corporation, New York, 1956.
- [2] Bermúdez, Y.G., Rico, I.L.R., Guibal, E., de Hoces, M.C. and Martín-Lara, M.Á., 2012. Biosorption of hexavalent chromium from aqueous solution by *Sargassum muticum* brown alga. Application of statistical design for process optimization. *Chemical Engineering Journal*, 183, pp.68-76.
- [3] Richard, F.C. and Bourg, A.C., 1991. Aqueous geochemistry of chromium: a review. *Water Research*, 25(7), pp.807-816.
- [4] Kotaś, J. and Stasicka, Z., 2000. Chromium occurrence in the environment and methods of its speciation. *Environmental pollution*, 107(3), pp.263-283.

- [5] Kirk-Othmer Encyclopedia of Chemical Technology (Vol. 8), Wiley, New York 1994.
- [6] Cieślak-Golonka, M., 1996. Toxic and mutagenic effects of chromium (VI). A review. *Polyhedron*, 15(21), pp.3667-3689.
- [7] Costa, M., 2003. Potential hazards of hexavalent chromate in our drinking water. *Toxicology and applied pharmacology*, 188(1), pp.1-5.
- [8] Miretzky, P. and Cirelli, A.F., 2010. Cr (VI) and Cr (III) removal from aqueous solution by raw and modified lignocellulosic materials: a review. *Journal of hazardous materials*, 180(1), pp.1-19.
- [9] Yang, L. and Chen, J.P., 2008. Biosorption of hexavalent chromium onto raw and chemically modified *Sargassum* sp. *Bioresource Technology*, 99(2), pp.297-307.
- [10] World Health Organization (WHO) Guidelines for drinking-water quality Recommendations, vol. 1, fourth ed., WHO, Geneva, 2011.
- [11] Dakiky, M., Khamis, M., Manassra, A. and Mer'eb, M., 2002. Selective adsorption of chromium (VI) in industrial wastewater using low-cost abundantly available adsorbents. *Advances in environmental research*, 6(4), pp.533-540.
- [12] Chen, Q., Hills, C.D., Yuan, M., Liu, H. and Tyrer, M., 2008. Characterization of carbonated tricalcium silicate and its sorption capacity for heavy metals: A micron-scale composite adsorbent of active silicate gel and calcite. *Journal of hazardous materials*, 153(1), pp.775-783.
- [13] Babel, S. and Kurniawan, T.A., 2003. Low-cost adsorbents for heavy metals uptake from contaminated water: a review. *Journal of hazardous materials*, 97(1), pp.219-243.
- [14] Guibal, E., 2004. Interactions of metal ions with chitosan-based sorbents: a review. *Separation and purification technology*, 38(1), pp.43-74.
- [15] Varma, A.J., Deshpande, S.V. and Kennedy, J.F., 2004. Metal complexation by chitosan and its derivatives: a review. *Carbohydrate Polymers*, 55(1), pp.77-93.
- [16] Krishnapriya, K.R. and Kandaswamy, M., 2010. A new chitosan biopolymer derivative as metal-complexing agent: synthesis, characterization, and metal (II) ion adsorption studies. *Carbohydrate research*, 345(14), pp.2013-2022.
- [17] Juang, R.S., Tseng, R.L., Wu, F.C. and Lee, S.H., 1997. Adsorption behavior of reactive dyes from aqueous solutions on chitosan. *Journal of Chemical Technology and Biotechnology*, 70(4), pp.391-399.
- [18] Chatterjee, S., Lee, M.W. and Woo, S.H., 2009. Enhanced mechanical strength of chitosan hydrogel beads by impregnation with carbon nanotubes. *Carbon*, 47(12), pp.2933-2936.
- [19] Miretzky, P. and Cirelli, A.F., 2009. Hg (II) removal from water by chitosan and chitosan derivatives: a review. *Journal of hazardous materials*, 167(1), pp.10-23.
- [20] Baraldi, P.G., Barbara, C., Giampiero, S., Romeo, R., Giovani, B., Abdel, N.Z., Pineda, D.L., 1998. *Synthesis*, pp.1140-1143.
- [21] Isloor, A.M., Kalluraya, B. and Shetty, P., 2009. Regioselective reaction: synthesis, characterization and pharmacological studies of some new Mannich bases derived from 1, 2, 4-triazoles. *European journal of medicinal chemistry*, 44(9), pp.3784-3787.
- [22] Kyzas, G.Z. and Deliyanni, E.A., 2013. Mercury (II) removal with modified magnetic chitosan adsorbents. *Molecules*, 18(6), pp.6193-6214.
- [23] Li, A., Lin, R., Lin, C., He, B., Zheng, T., Lu, L. and Cao, Y., 2016. An environment-friendly and multi-functional adsorbent from chitosan for organic pollutants and heavy metal ion. *Carbohydrate polymers*, 148, pp.272-280.
- [24] Webster, A., Halling, M.D. and Grant, D.M., 2007. Metal complexation of chitosan and its glutaraldehyde cross-linked derivative. *Carbohydrate Research*, 342(9), pp.1189-1201.
- [25] Hussein, M.H., El-Hady, M.F., Sayed, W.M. and Hefni, H., 2012. Preparation of some chitosan heavy metal complexes and study of its properties. *Polymer Science Series A*, 54(2), pp.113-124.
- [26] Jin, X., Wang, J. and Bai, J., 2009. Synthesis and antimicrobial activity of the Schiff base from chitosan and citral. *Carbohydrate research*, 344(6), pp.825-829.
- [27] Chethan, P.D. and Vishalakshi, B., 2015. Synthesis of ethylenediamine modified chitosan microspheres for removal of divalent and hexavalent ions. *International journal of biological macromolecules*, 75, pp.179-185.
- [28] Ngah, W.S.W., Kamari, A., Fatimathan, S. and Ng, P.W., 2006. Adsorption of chromium from aqueous solution using chitosan beads. *Adsorption*, 12(4), pp.249-257.
- [29] Kyzas, G.Z., Kostoglou, M. and Lazaridis, N.K., 2009. Copper and chromium (VI) removal by chitosan derivatives—Equilibrium and kinetic

- studies. *Chemical Engineering Journal*, 152(2), pp.440-448.
- [30] Chauhan, D., Jaiswal, M. and Sankararamkrishnan, N., 2012. Removal of cadmium and hexavalent chromium from electroplating waste water using thiocarbamoyl chitosan. *Carbohydrate Polymers*, 88(2), pp.670-675.
- [31] Qin, C., Du, Y., Zhang, Z., Liu, Y., Xiao, L. and Shi, X., 2003. Adsorption of chromium (VI) on a novel quaternized chitosan resin. *Journal of applied polymer science*, 90(2), pp.505-510.
- [32] Zhang, L., Zeng, Y. and Cheng, Z., 2016. Removal of heavy metal ions using chitosan and modified chitosan: A review. *Journal of Molecular Liquids*, 214, pp.175-191.
- [33] Foo, S.K. and Hameed, B.H., 2010. Insights into the modeling of adsorption isotherm systems. *Chemical Engineering Journal*, 156(1), pp.2-10.
- [34] Liao, B., Sun, W.Y., Guo, N., Ding, S.L. and Su, S.J., 2016. Equilibriums and kinetics studies for adsorption of Ni (II) ion on chitosan and its triethylenetetramine derivative. *Colloids and Surfaces A: Physicochemical and Engineering Aspects*, 501, pp.32-41.
- [35] Zarghami, Z., Akbari, A., Latifi, A.M. and Amani, M.A., 2016. Design of a new integrated chitosan-PAMAM dendrimer biosorbent for heavy metals removing and study of its adsorption kinetics and thermodynamics. *Bioresource technology*, 205, pp.230-238.
- [36] Anandkumar, J. and Mandal, B., 2009. Removal of Cr (VI) from aqueous solution using Bael fruit (*Aegle marmelos* correa) shell as an adsorbent. *Journal of hazardous materials*, 168(2), pp.633-640.
- [37] Sharma, A. and Bhattacharyya, K.G., 2005. Adsorption of chromium (VI) on *Azadirachta indica* (Neem) leaf powder. *Adsorption*, 10(4), pp.327-338.
- [38] Garg, U.K., Kaur, M.P., Garg, V.K. and Sud, D., 2007. Removal of hexavalent chromium from aqueous solution by agricultural waste biomass. *Journal of Hazardous Materials*, 140(1), pp.60-68.
- [39] Zhang, R., Wang, B. and Ma, H., 2010. Studies on Chromium (VI) adsorption on sulfonated lignite. *Desalination*, 255(1), pp.61-66.
- [40] Liao, X.P., Tang, W., Zhou, R.Q. and Shi, B., 2008. Adsorption of metal anions of vanadium (V) and chromium (VI) on Zr (IV)-impregnated collagen fiber. *Adsorption*, 14(1), pp.55-64.
- [41] Dai, B., Cao, M., Fang, G., Liu, B., Dong, X., Pan, M. and Wang, S., 2012. Schiff base-chitosan grafted multiwalled carbon nanotubes as a novel solid-phase extraction adsorbent for determination of heavy metal by ICP-MS. *Journal of hazardous materials*, 219, pp.103-110.
- [42] Kousalya, G.N., Gandhi, M.R. and Meenakshi, S., 2010. Sorption of chromium (VI) using modified forms of chitosan beads. *International Journal of Biological Macromolecules*, 47(2), pp.308-315.
- [43] Udaybhaskar, P., Iyengar, L. and Rao, A.V.S., 1990. Hexavalent chromium interaction with chitosan. *Journal of Applied Polymer Science*, 39(3), pp.739-747.
- [44] Hu, X.J., Wang, J.S., Liu, Y.G., Li, X., Zeng, G.M., Bao, Z.L., Zeng, X.X., Chen, A.W. and Long, F., 2011. Adsorption of chromium (VI) by ethylenediamine-modified cross-linked magnetic chitosan resin: isotherms, kinetics and thermodynamics. *Journal of hazardous materials*, 185(1), pp.306-314.
- [45] Sun, X., Peng, B., Ji, Y., Chen, J. and Li, D., 2009. Chitosan (chitin)/cellulose composite biosorbents prepared using ionic liquid for heavy metal ions adsorption. *AIChE journal*, 55(8), pp.2062-2069.
- [46] Ferrero, F., Tonetti, C. and Periolatto, M., 2014. Adsorption of chromate and cupric ions onto chitosan-coated cotton gauze. *Carbohydrate polymers*, 110, pp.367-373.
- [47] Tseng, R.L., Wu, F.C. and Juang, R.S., 2003. Liquid-phase adsorption of dyes and phenols using pinewood-based activated carbons. *Carbon*, 41(3), pp.487-495.
- [48] Wang, X. and Wang, C., 2016. Chitosan-poly (vinyl alcohol)/attapulgitite nanocomposites for copper (II) ions removal: pH dependence and adsorption mechanisms. *Colloids and Surfaces A: Physicochemical and Engineering Aspects*, 500, pp.186-194.
- [49] Janciauskaite, U., Rakutyte, V., Miskinis, J. and Makuska, R., 2008. Synthesis and properties of chitosan-N-dextran graft copolymers. *Reactive and Functional Polymers*, 68(3), pp.787-796.